Influence of O_2 and N_2 on the conductivity of carbon nanotube networks

D. J. Mowbray,[1,*] C. Morgan,[2] and K. S. Thygesen[1]
[1]*Department of Physics, Center for Atomic-scale Materials Design (CAMD), Technical University of Denmark, DK-2800 Kgs. Lyngby, Denmark*
[2]*Department of Physics, Molecular and Materials Physics Group, Queen Mary University of London, Mile End Road, London E1 4NS, United Kingdom*
(Received 11 February 2009; published 22 May 2009)

We have performed experiments on single-wall carbon nanotube (SWNT) networks and compared with density-functional theory (DFT) calculations to identify the microscopic origin of the observed sensitivity of the network conductivity to physisorbed O_2 and N_2. Previous DFT calculations of the transmission function for isolated pristine SWNTs have found physisorbed molecules have little influence on their conductivity. However, by calculating the four-terminal transmission function of crossed SWNT junctions, we show that physisorbed O_2 and N_2 do affect the junction's conductance. This may be understood as an increase in tunneling probability due to hopping via molecular orbitals. We find the effect is substantially larger for O_2 than for N_2, and for semiconducting rather than metallic SWNTs junctions, in agreement with experiment.

DOI: 10.1103/PhysRevB.79.195431 PACS number(s): 73.63.−b, 68.43.−h, 73.50.Lw

I. INTRODUCTION

Using single-wall carbon nanotubes (SWNTs) as nanosensors, both individually and in SWNT networks, has been one of the most promising potential applications of SWNTs since their discovery.[1,2] Several experimental studies have demonstrated that the conductance of SWNT systems is rather sensitive to the presence of even single-molecule concentrations of physisorbed gas molecules such as O_2 and N_2.[3–9] Further, by measuring conductivity of individually characterized SWNTs,[10] as well as thick (metal-like) and thin (semiconductorlike) SWNT networks,[8,9,11] the response of SWNTs to contaminants has been shown to correlate with the intrinsic electronic properties of the material. For example, it has been found that the presence of low-O_2 concentrations, independent of temperature, introduces an increase in conductance of approximately 20% on thin SWNT networks while an increase in conductance of only about 1% is found for thick SWNT networks.[8]

On the other hand, previous theoretical studies have found that SWNTs are rather inert so that gases tend only to physisorb to the SWNT surface.[12–19] For this reason it was suggested that O_2 should not effect conductance through SWNTs but only influence conductance at either SWNT-SWNT junctions, at the SWNT-metal contacts, or at SWNT defect sites.[12,20] Although the conductivity of SWNTs with molecules physisorbed at defect sites has been extensively studied,[21–23] the conductivity of four-terminal SWNT-SWNT junctions has been previously studied only for small pristine metallic SWNTs.[24,25] The possible influence of physisorbed molecules on SWNT-SWNT junctions has not been investigated.

In this paper we address the microscopic origin of the increase in conductance of SWNT networks when exposed to O_2 or N_2 gas. To this end, we have performed density-functional theory (DFT) calculations of the intratube transmission within a SWNT and the intertube transmission between two SWNTs in the nonequilibrium Green's function (NEGF) formalism for O_2 and N_2 molecules physisorbed in (7,7) metallic armchair, (12,0) semimetallic zigzag, and (13,0) semiconducting zigzag SWNT junctions, shown schematically in Fig. 1. Comparing our theoretical results for SWNT junctions with experimental measurements for SWNT networks suggests that the surprising sensitivity to O_2 and N_2 may be partially due to an increased tunneling probability through O_2 and N_2 physisorbed at SWNT junctions.

In Sec. II we describe experimental measurements of the influence of both O_2 and N_2 on the conductivity of SWNT networks and the characterization of these networks using Raman spectroscopy. A description of the DFT and NEGF model used to describe the microscopic origin of this effect is then provided in Sec. III. In Sec. IV we compare our theoretical results for the SWNT junction transmission with the SWNT network experiments followed by a concluding section.

II. EXPERIMENTAL RESULTS

Below we give a brief discussion of our experiments on SWNT network conductivity. A more detailed description

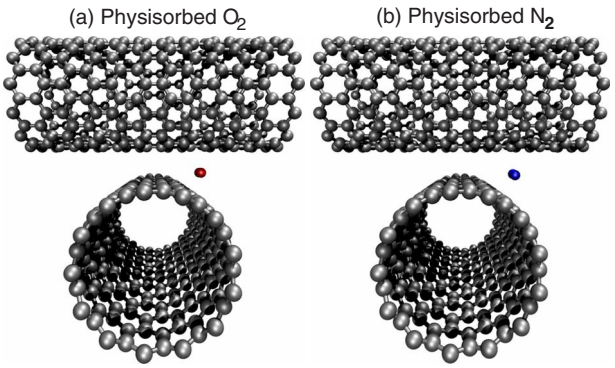

FIG. 1. (Color online) Schematics of a (13,0) SWNT junction with (a) physisorbed O_2 and (b) physisorbed N_2.

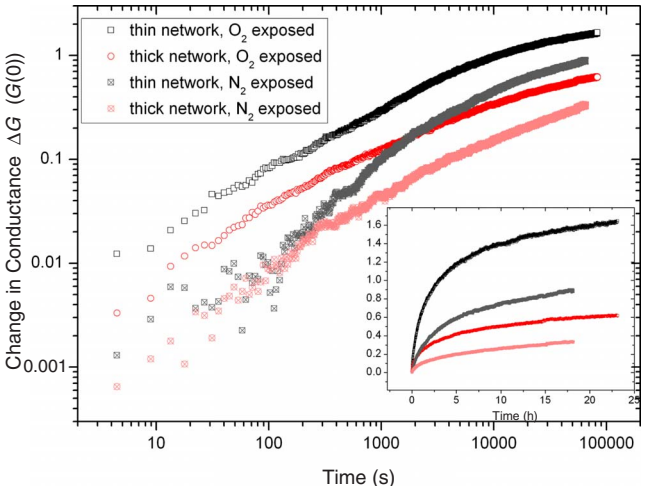

FIG. 2. (Color online) Fractional change in conductance $\Delta G = G/G(0) - 1$ versus time t in seconds and hours (inset) following exposure to O_2 and N_2 for thin (□,⊠) and thick (○,⊗) SWNT networks, respectively, on log-log and linear (inset) scales (Refs. 8 and 9).

may be found in Refs. 8 and 9. Figure 2 shows experimental measurements of the conductance sensitivity to O_2 and N_2 exposure for thick and thin SWNT networks. These samples were initially placed under vacuum ($\sim 1 \times 10^{-6}$ mbar) and irradiated by a UV light-emitting diode (LED) ($\lambda \sim 400$ nm) at low intensity (~ 0.03 mW/cm^2) for approximately 12 h to desorb surface and interbundle adsorbates (surface dopants) from the SWNTs. Once the SWNT network's conductance stabilized, the samples were exposed to either O_2 (99.5% pure) or N_2 (99.998% pure) at 1 atm. The conductance of the samples was then monitored by periodically sampling ($\Delta t \approx 1$ s) the current while applying a fixed bias of 1 mV to the thick (metal-like) SWNT network ($R \approx 1$ kΩ) and 10 mV to the thin (semiconductorlike) SWNT network ($R \approx 1000$ kΩ), as shown in Fig. 2.

After 5 min of exposure to O_2, the thin network shows an increase in conductance of about 13% while the thick network's conductance changes by about 7%. For the same exposure to N_2, both networks show substantially smaller conductance changes of 2%–3%. However, at exposure times of more than 2 h, the thin SWNT network response to N_2 is similar to that of the thick SWNT network to O_2. This might be caused by a weaker physisorption of N_2 to the SWNT networks than O_2. The inset of Fig. 2 also shows that at very long exposure times the fractional change in conductance, $\Delta G = G/G(0) - 1$, becomes saturated after 24 h. Further, the response to O_2 depicted in Fig. 2 shows that the conductance change for a thin SWNT network is about two to three times that of the thick SWNT network at all times. This suggests that the conductance change under O_2 exposure is an intrinsic property of the SWNT networks present even at very low O_2 concentrations. Herein we shall focus on the microscopic origin of the network sensitivity to O_2 and N_2 with the temporal behavior of the networks discussed elsewhere.[8,9]

We have performed the Raman spectroscopy to characterize our SWNT network samples, which were produced via the high-pressure carbon monoxide (HiPco) method. Figure

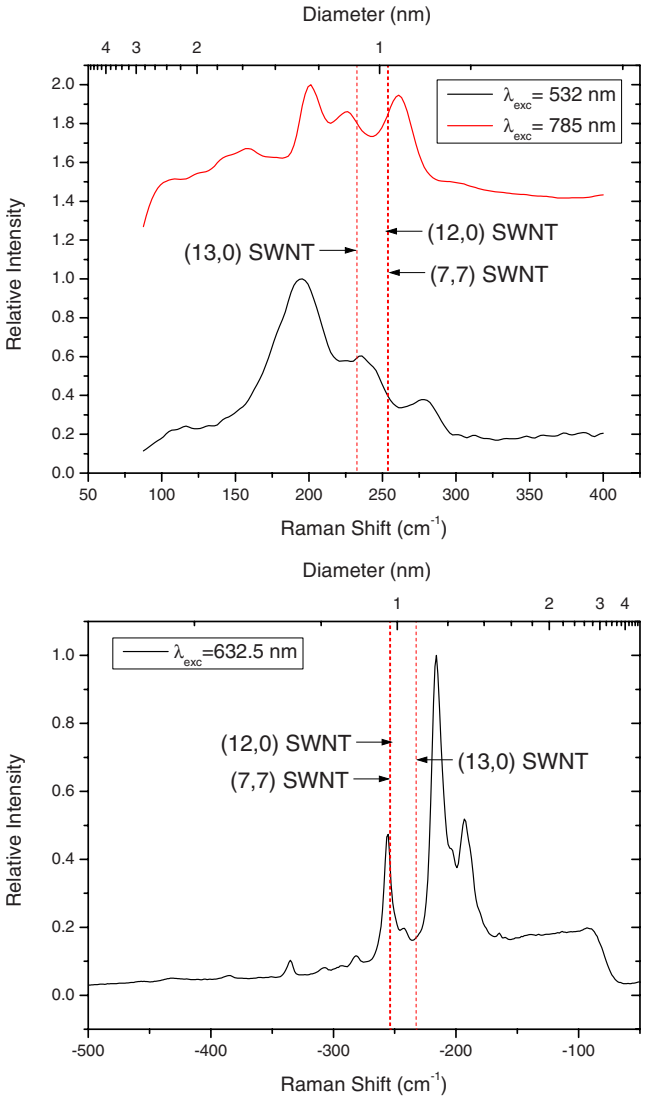

FIG. 3. (Color online) Raman spectra and approximate diameter distribution of HiPco SWNT sample for an excitation wavelength (top) $\lambda_{exc} \approx 532$ nm (lower black curve), $\lambda_{exc} \approx 785$ nm (upper red curve), and (bottom) $\lambda_{exc} \approx 632.5$ nm. The DFT calculated diameters of $d \approx 9.76$ Å, 9.79 Å, and 10.66 Å for (7,7), (12,0), and (13,0) SWNTs, respectively, are provided for comparison (dashed lines).

3 shows the radial breathing mode (RBM) Raman signals of HiPco samples at excitation wavelengths $\lambda_{exc} \approx 532$ nm, $\lambda_{exc} \approx 632.5$ nm, and $\lambda_{exc} \approx 785$ nm. The van Hove singularity energy separation was calculated using the tight-binding approximation with the carbon-carbon interaction energy $\gamma_0 \approx 2.9$ eV and carbon-carbon bond length $a_{C\text{-}C} \approx 1.44$ Å. The SWNT diameter d dependence of the RBM frequency ν_{RBM} for isolated SWNTs on SiO_2 has been shown[26] to behave as $\nu_{RBM} \approx 248/d_t$. The DFT calculated diameters for (7,7), (12,0), and (13,0) SWNTs of $d \approx 9.76$, 9.79, and 10.66 Å, respectively, are found to correlate well with the HiPco Raman shift, as shown in Fig. 3. This should ensure a good description of the SWNT network's work function, which may be significantly different for smaller tubes.

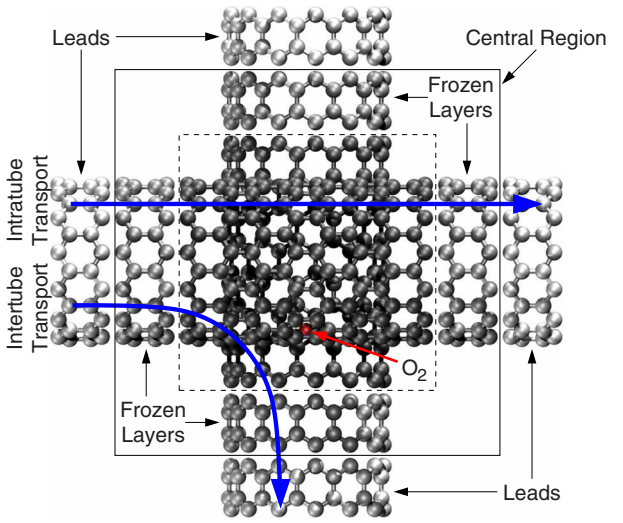

FIG. 4. (Color online) Schematic of (13,0) SWNT junction consisting of four SWNT leads (light gray) coupled to the central scattering region via four SWNT primitive unit cells or layers (gray) "frozen" at their relative positions in the isolated SWNT. The atomic positions of the remaining eight SWNT layers (dark gray) and the physisorbed O_2 molecule have been relaxed. A SWNT separation consistent with experiments of approximately 3.4 Å has been used. The intratube transport through the SWNT and the intertube transport between the SWNTs has been shown schematically.

III. BASIC THEORY

Our DFT calculations have been performed with the SIESTA DFT code[27,28] using a double-zeta polarized (DZP) basis set for the physisorbed molecules (O and N), and a single-zeta polarized (SZP) basis set for the SWNTs (C), and the Perdew-Burke-Ernzerhof (PBE) exchange-correlation functional.[29] We note here that the DZP and SZP SIESTA basis sets have recently been shown to yield transmission functions in quantitative agreement with plane-wave codes and maximally localized Wannier functions.[30] When modeling O_2 we have performed spin-polarized calculations[12] but have performed spin-unpolarized calculations otherwise.

We have modeled the junction system using 6(11) primitive unit cells or layers for each zigzag(armchair) SWNT per supercell, with a separation of approximately 3.4 Å, as depicted for a (13,0) SWNT junction in Figs. 1 and 4.[31] The four SWNT layers at the boundaries of the central region, shown in gray in Fig. 4, were kept fixed at their relaxed positions in the isolated SWNT. At the same time the central 4(9) primitive unit cells from each tube, shown in dark gray in Fig. 4, and the physisorbed molecules were relaxed until a maximum force of less than 0.1 eV/Å was obtained. Since the supercell has dimensions of $\gtrsim$25 Å for each SWNT junction, a Γ point calculation was sufficient to describe the periodicity of the structure.

Such a large supercell was necessary for the Hamiltonian of each of the four SWNT layers adjacent to the boundaries H_C^{prin}, to be within 0.1 eV of the Hamiltonian for the respective leads H_α, so that $\max|H_C^{\text{prin}}-H_\alpha|<0.1$ eV. In this way the electronic structure at the edges of the central region was ensured to be converged to that in the leads.

TABLE I. Change in intertube conductance ΔG_{inter} at the valence-band maximum ε_{VB} relative to the pristine junction for O_2 and N_2 physisorbed in SWNT junctions of (7,7), (12,0), and (13,0) SWNTs, with the respective SWNT-O_2 and SWNT-N_2 separations d in Angstrom.

	ΔG_{inter} (%)		d [Å]	
SWNT junction	O_2	N_2	SWNT–O_2	SWNT–N_2
(7,7) Armchair	30	6	2.3	2.8
(12,0) Zigzag	140	14	2.6	2.8
(13,0) Zigzag	1800	130	2.5	2.8

The Landauer-Bütticker conductance for a multiterminal system can be calculated from the Green's function of the central region, G_C, according to the formula[32–34]

$$G = G_0\,\mathrm{Tr}[G_C\Gamma_{\text{in}}G_C^\dagger\Gamma_{\text{out}}]|_{\varepsilon=\varepsilon_F}, \tag{1}$$

where the trace runs over all localized basis functions in the central region. To describe the conductance at small bias for semiconducting systems, the Fermi energy ε_F should be taken as the energy of the valence-band maximum ε_{VB} or conduction-band minimum ε_{CB} for p-type and n-type semiconductors, respectively. The central region Green's function is calculated from

$$G_C(\varepsilon) = \left[zS_C - H_C - \sum_\alpha \Sigma_\alpha(\varepsilon)\right]^{-1}, \tag{2}$$

where $z=\varepsilon+i0^+$, S_C and H_C are the overlap matrix and Kohn-Sham Hamiltonian matrix of the central region in the localized basis, Σ_α is the self-energy of lead α,

$$\Sigma_\alpha(\varepsilon) = [zS_{C\alpha} - H_{C\alpha}][zS_\alpha - H_\alpha]^{-1}[zS_{C\alpha}^\dagger - H_{C\alpha}^\dagger], \tag{3}$$

and the coupling elements between the central region and lead α for the overlap and Kohn-Sham Hamiltonian are $S_{C\alpha}$ and $H_{C\alpha}$, respectively.

The coupling strengths of the input and output leads are then given by $\Gamma_{\text{in/out}}=i(\Sigma_{\text{in/out}}-\Sigma_{\text{in/out}}^\dagger)$. For a four-terminal SWNT junction, the intratube and intertube transmission functions are calculated by choosing the appropriate output lead, as depicted in Fig. 4.

IV. THEORETICAL RESULTS AND DISCUSSION

For each of the three types of SWNT junctions considered we find that both O_2 and N_2 are physisorbed with binding energies of $\sim$0.2 eV, as depicted in Fig. 1. Further, the SWNT-O_2 and SWNT-N_2 equilibrium separation distance d is in the range 2.3–2.8 Å, as given in Table I. These results agree qualitatively with previous theoretical studies for O_2 binding distances and energies on isolated SWNTs.[12–19]

Figures 5(a)–5(c) show the intratube transmission for three prototypical SWNTs commonly found in experimental HiPco samples,[35] as shown in Fig. 3. In Fig. 5(a) we see that for a metallic armchair (7,7) SWNT, transmission occurs through two channels at the Fermi level. We see in Fig. 5(b)

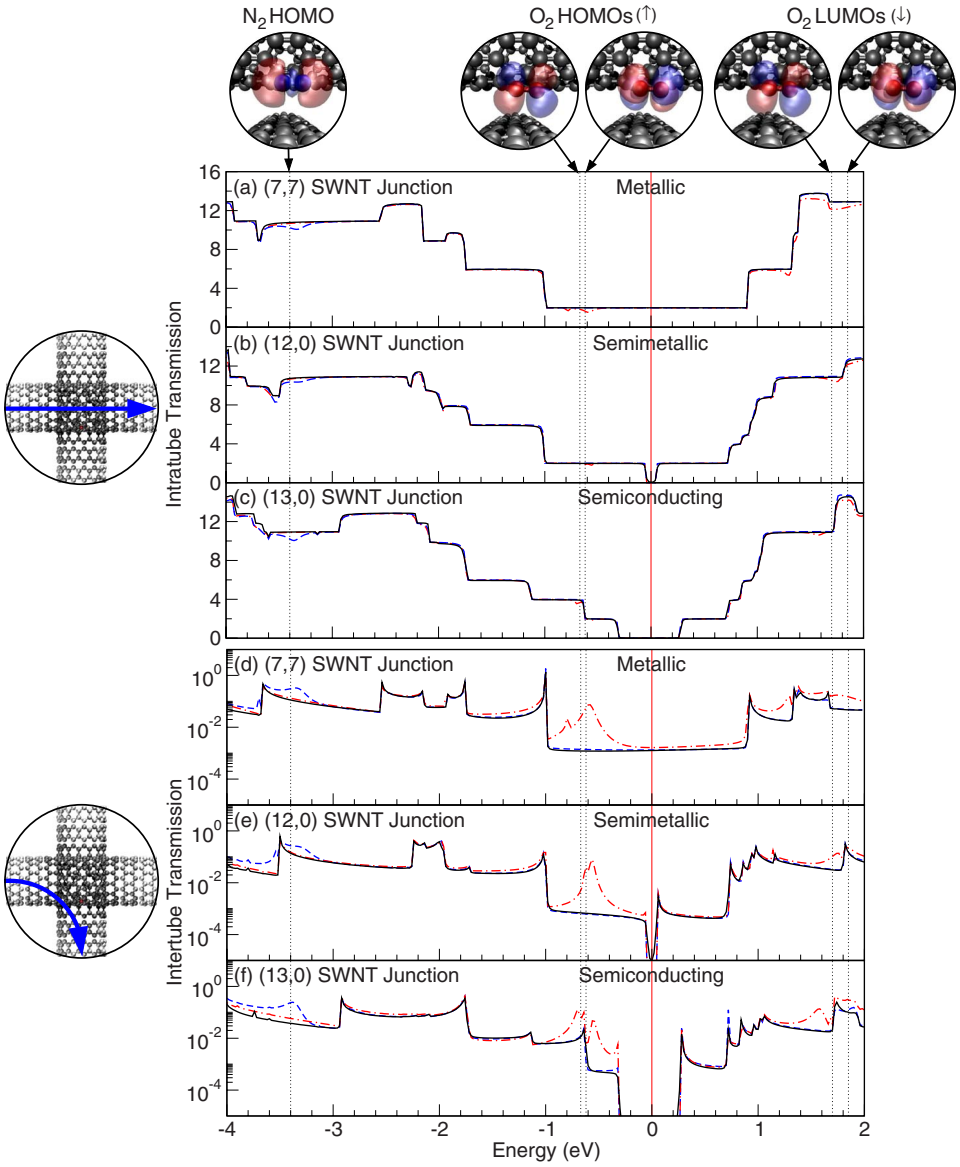

FIG. 5. (Color online) (a)–(c) Intratube transmission and (d)–(f) intertube transmission vs energy in eV relative to the Fermi energy for a pristine (black solid lines) SWNT junction, and with N_2 (blue dashed lines), and O_2 (red dash-dotted lines) physisorbed consisting of [(a) and (d)] metallic (7,7) SWNTs, [(b) and (e)] semimetallic (12,0) SWNTs, and [(c) and (f)] semiconducting (13,0) SWNTs. Schematics and isosurfaces of $\pm 0.02\ e/\mathrm{A}^3$ for molecular orbitals on the physisorbed molecules are shown above the corresponding eigenenergies (dotted lines).

that the conductance for the semimetallic zigzag (12,0) SWNT resembles that found in Fig. 5(a) for a metallic SWNT, except for a tiny band gap of $\lesssim 0.05$ eV at the Fermi level. In Fig. 5(c) we find for a semiconducting zigzag (13,0) SWNT a band gap of approximately 0.6 eV between the valence and conduction bands through which no transmission occurs. This is only slightly smaller than the expected band gap of ~ 0.7 eV based on a d^{-1} fit to experimental data.[36] These results for the intratube transmission of pristine SWNTs also agree qualitatively with previous DFT studies of isolated (5,5), (10,10), (10,5), (11,0), and (12,0) SWNTs.[25,37,38] We also find in Figs. 5(a)–5(c) that neither O_2 nor N_2 physisorbed at a SWNT junction noticeably influence the intratube transmission.

In Fig. 5 we also show isosurfaces and eigenenergies for the highest occupied and lowest occupied molecular orbitals (HOMO and LUMO) on physisorbed O_2 and N_2. For these weakly coupled molecules, the renormalized molecular levels may easily be identified with the molecular orbitals of the free O_2 and N_2 molecules.[39] Since the position of the molecular levels is rather insensitive to the type of junction, it should also be insensitive to the exact binding geometry. This suggests that additional physisorbed molecules will influence the intertube transmission similarly.

We find the intertube transmission is proportional to the density of states (DOS) for the system with peaks in the transmission at the van Hove singularities. This is consistent with transport between the SWNTs occurring in the tunnel-

ing regime, as expected for a SWNT separation of approximately 3.4 Å.

The presence of physisorbed molecules in the SWNT-SWNT gap should then increase the tunneling probability at energies near the eigenenergies of the molecular orbitals. This is evidenced by the distinct peaks in the intertube transmission for each SWNT junction at energies corresponding to the HOMO of N_2 and the spin-polarized HOMOs and LUMOs of O_2, as seen in Figs. 5(d)–5(f). Under such conditions, a SWNT junction behaves as a simple tunneling electron microscopy (TEM) tip. By applying appropriate bias voltages, one may potentially probe the molecular orbitals of a physisorbed molecule to determine its chemical composition.

For this reason, the sensitivity of SWNT network conductivity to O_2 is at least partly due to the close proximity of the O_2 HOMOs to the Fermi energies of typical SWNTs ($\approx$0.6 eV), as shown in Fig. 5. Further, it has been shown experimentally that defects inherent in physically realizable SWNTs yield *p*-type semiconductors.[1,40,41] The conductivity measured experimentally at small bias is thus at the energy of the valence band ε_{VB}.

As seen in Fig. 5(f), the O_2 HOMO eigenenergy is only about 0.3 eV below ε_{VB} for a semiconducting (13,0) SWNT junction. As shown in Table I, this yields a substantial increase in the intertube conductance at zero bias for semiconducting junctions in the presence of O_2 while much smaller increases are found for the metallic and semimetallic junctions in agreement with experiment.[8] On the other hand, we also find physisorbed N_2 increases the intertube conductance only slightly, also in qualitative agreement with experiment,[5] as shown in Fig. 2.

Although it is well-known DFT calculations underestimate band gaps[37,42,43] since we are primarily interested in how the presence of O_2 or N_2 qualitatively changes the DOS and conductance, such calculations are still useful.

V. CONCLUSIONS

In conclusion, we have proposed a possible microscopic explanation for the experimentally observed sensitivity of the electrical conductance of carbon nanotube networks to oxygen and nitrogen gases. Our DFT calculations suggest that O_2 and N_2 physisorbed in crossed SWNT junctions can have a large influence on the intertube conductance. In particular, for O_2 the close proximity of the highest occupied molecular orbitals with the Fermi level of the SWNT significantly increases electron tunneling across the gap. The effect is found to be larger for O_2 than for N_2 and for semiconducting rather than metallic SWNTs, in agreement with the experimental observations. Our results suggest that the electrical properties of SWNT networks are to a large extent determined by crossed SWNT junctions.

ACKNOWLEDGMENTS

We thank E. I. Kauppinen, and K. W. Jacobson for useful discussions. D.J.M. and K.S.T. acknowledge financial support from NABIIT and the Danish Center for Scientific Computing under Grant No. HDW-1103-06. The Center for Atomic-scale Materials Design (CAMD) is sponsored by the Lundbeck Foundation. C.M. acknowledges financial support from the National Physical Laboratory (NPL) and the Engineering and Physical Sciences Research Council (EPSRC-GB).

*dmowbray@fysik.dtu.dk

[1] *Carbon Nanotubes: Sythesis, Structure, Properties, and Applications*, edited by M. S. Dresselhaus, G. Dresselhaus, and P. Avouris (Springer, Berlin, 2001).
[2] D. R. Kauffman and A. Star, Angew. Chem. **47**, 6550 (2008).
[3] K. Bradley, S.-H. Jhi, P. G. Collins, J. Hone, M. L. Cohen, S. G. Louie, and A. Zettl, Phys. Rev. Lett. **85**, 4361 (2000).
[4] P. G. Collins, K. Bradley, M. Ishigami, and A. Zettl, Science **287**, 1801 (2000).
[5] G. U. Sumanasekera, C. K. W. Adu, S. Fang, and P. C. Eklund, Phys. Rev. Lett. **85**, 1096 (2000).
[6] A. Felten, J. Ghijsen, J.-J. Pireaux, R. L. Johnson, C. M. Whelan, D. Liang, G. V. Tendeloo, and C. Bittencourt, J. Phys. D **40**, 7379 (2007).
[7] M. Kaempgen, M. Lebert, M. Haluska, N. Nicoloso, and S. Roth, Adv. Mater. **20**, 616 (2008).
[8] C. Morgan, Z. Alemipour, and M. Baxendale, Phys. Status Solidi A **205**, 1394 (2008).
[9] C. Morgan and M. Baxendale, arXiv:0905.1821v1 (unpublished).
[10] J. Kong, N. R. Franklin, C. Zhou, M. G. Chapline, S. Peng, K. Cho, and H. Dai, Science **287**, 622 (2000).
[11] V. Skákalová, A. B. Kaiser, Y.-S. Woo, and S. Roth, Phys. Rev. B **74**, 085403 (2006).
[12] P. Giannozzi, R. Car, and G. Scoles, J. Chem. Phys. **118**, 1003 (2003).
[13] A. Tchernatinsky, S. Desai, G. U. Sumanasekera, C. S. Jayanthi, S. Y. Wu, B. Nagabhirava, and B. Alphenaar, J. Appl. Phys. **99**, 034306 (2006).
[14] V. A. Margulis and E. E. Muryumin, Phys. Rev. B **75**, 035429 (2007).
[15] S. Peng and K. Cho, Nanotechnology **11**, 57 (2000).
[16] D. C. Sorescu, K. D. Jordan, and P. Avouris, J. Phys. Chem. B **105**, 11227 (2001).
[17] D. J. Mann and W. L. Hase, Phys. Chem. Chem. Phys. **3**, 4376 (2001).
[18] S.-H. Jhi, S. G. Louie, and M. L. Cohen, Phys. Rev. Lett. **85**, 1710 (2000).
[19] S.-P. Chan, G. Chen, X. G. Gong, and Z.-F. Liu, Phys. Rev. Lett. **90**, 086403 (2003).
[20] A. R. Rocha, M. Rossi, A. Fazzio, and A. J. R. da Silva, Phys. Rev. Lett. **100**, 176803 (2008).
[21] S. Peng and K. Cho, Nano Lett. **3**, 513 (2003).
[22] P. C. P. Watts, N. Mureau, Z. Tang, Y. Miyajima, J. D. Carey, and S. R. P. Silva, Nanotechnology **18**, 175701 (2007).
[23] P. C. P. Watts, W.-K. Hsu, H. W. Kronto, and D. R. M. Walton,

Nano Lett. **3**, 549 (2003).
[24] M. S. Fuhrer, J. Nygård, L. Shih, M. Forero, Y.-G. Yoon, M. S. C. Mazzoni, H. J. Choi, J. Ihm, S. G. Louie, A. Zettl, and, P. L. McEuen, Science **288**, 494 (2000).
[25] Y.-G. Yoon, M. S. C. Mazzoni, H. J. Choi, J. Ihm, and S. G. Louie, Phys. Rev. Lett. **86**, 688 (2001).
[26] A. Jorio, R. Saito, J. H. Hafner, C. M. Lieber, M. Hunter, T. McClure, G. Dresselhaus, and M. S. Dresselhaus, Phys. Rev. Lett. **86**, 1118 (2001).
[27] S. R. Bahn and K. W. Jacobsen, Comput. Sci. Eng. **4**, 56 (2002).
[28] J. M. Soler, E. Artacho, J. D. Gale, A. Garcia, J. Junquera, P. Ordejón, and D. Sánchez-Portal, J. Phys.: Condens. Matter **14**, 2745 (2002).
[29] J. P. Perdew, K. Burke, and M. Ernzerhof, Phys. Rev. Lett. **77**, 3865 (1996).
[30] M. Strange, I. S. Kristensen, K. S. Thygesen, and K. W. Jacobsen, J. Chem. Phys. **128**, 114714 (2008).
[31] J. Kleis, P. Hyldgaard, and E. Schröder, Comput. Mater. Sci. **33**, 192 (2005).
[32] Y. Meir and N. S. Wingreen, Phys. Rev. Lett. **68**, 2512 (1992).
[33] K. S. Thygesen, Phys. Rev. B **73**, 035309 (2006).
[34] M. Buttiker, Phys. Rev. Lett. **57**, 1761 (1986).
[35] Z. Luo, L. D. Pfefferle, G. I. Haller, and F. Papadimitrakopoulos, J. Am. Chem. Soc. **128**, 15511 (2006).
[36] T. W. Odom, J.-L. Huang, P. Kim, and C. M. Lieber, J. Phys. Chem. B **104**, 2794 (2000).
[37] S. Reich, C. Thomsen, and P. Ordejón, Phys. Rev. B **65**, 155411 (2002).
[38] J.-C. Charlier, X. Blase, and S. Roche, Rev. Mod. Phys. **79**, 677 (2007).
[39] K. S. Thygesen and K. W. Jacobsen, Chem. Phys. **319**, 111 (2005).
[40] S. Tans, A. Vershueren, and C. Dekker, Nature (London) **393**, 49 (1998).
[41] V. Derycke, R. Martel, J. Appenzeller, and P. Avouris, Nano Lett. **1**, 453 (2001).
[42] J. Paier, M. Marsman, K. Hummer, G. Kresse, I. C. Gerber, and J. G. Angyan, J. Chem. Phys. **124**, 154709 (2006).
[43] J. Heyd, J. E. Peralta, G. E. Scuseria, and R. L. Martin, J. Chem. Phys. **123**, 174101 (2005).